



1 **Mass spectrometric measurement of hydrogen isotope fractionation for the**  
2 **reactions of chloromethane with OH and Cl**

3

4 **Frank Keppler<sup>1,2,3</sup>, Enno Bahlmann<sup>4,5</sup>, Markus Greule<sup>1,3</sup>, Heinz Friedrich Schöler<sup>1</sup>**  
5 **Julian Wittmer<sup>6,7</sup> and Cornelius Zetzsch<sup>3,6</sup>**

6 [1] Institute of Earth Sciences, Heidelberg University, Im Neuenheimer Feld 234-236, 69120  
7 Heidelberg, Germany

8 [2] Heidelberg Center for the Environment (HCE), Heidelberg University, D-69120  
9 Heidelberg, Germany

10 [3] Max-Planck-Institute for Chemistry, Hahn-Meitner-Weg 1, 55128 Mainz, Germany

11 [4] Leibniz Centre for Tropical Marine Research, Fahrenheitstraße 6, 28359 Bremen

12 [5] Institute of Geology, University Hamburg, Bundesstrasse 55, 20146 Hamburg, Germany

13 [6] Atmospheric Chemistry Research Unit, BayCEER, University of Bayreuth, Dr Hans-  
14 Frisch Strasse 1-3, D-95448 Bayreuth, Germany.

15 [7] Agilent Technologies Sales & Services GmbH & Co. KG, Hewlett-Packard-Str. 8, 76337  
16 Waldbronn, Germany

17 Correspondence to: Frank Keppler ([frank.keppler@geow.uni-heidelberg.de](mailto:frank.keppler@geow.uni-heidelberg.de))

18

19 **Abstract**

20 Chloromethane (CH<sub>3</sub>Cl) is an important provider of chlorine to the stratosphere but yet lacks  
21 detailed knowledge of its budget. Stable isotope analysis is potentially a powerful tool to  
22 constrain CH<sub>3</sub>Cl flux estimates. The largest degree of isotope fractionation is expected to  
23 occur for deuterium in CH<sub>3</sub>Cl in the hydrogen abstraction reactions with its main sink  
24 reactant tropospheric OH and its minor sink reactant Cl atoms. We determined the isotope  
25 fractionation by stable hydrogen isotope analysis of the fraction of CH<sub>3</sub>Cl remaining after  
26 reaction with hydroxyl and chlorine radicals in a 3.5 m<sup>3</sup> Teflon smog-chamber at 293 ± 1K.  
27 We measured the increasing stable hydrogen isotope values of the unreacted CH<sub>3</sub>Cl using  
28 compound specific thermal conversion isotope ratio mass spectrometry. The isotope  
29 fractionations of CH<sub>3</sub>Cl for the reactions with hydroxyl and chlorine radicals were found to  
30 be -242 ± 7 mUr (or ‰) and -280 ± 11 mUr, respectively. For comparison, we performed



31 similar experiments using methane ( $\text{CH}_4$ ) as the target compound with OH and obtained a  
32 fractionation constant of  $-205 \pm 6$  mUr which is in good agreement with values previously  
33 reported. The observed large kinetic isotope effects are helpful when employing isotopic  
34 analyses of  $\text{CH}_3\text{Cl}$  in the atmosphere to improve our knowledge of its atmospheric budget.

35

## 36 1 Introduction

37 Chloromethane (often named methyl chloride) is the most abundant chlorine containing trace  
38 gas in the Earth's atmosphere, currently with a global mean mixing ratio of  $\sim 540 \pm 5$  parts  
39 per trillion by volume (pptv) and an atmospheric lifetime of 1.0–1.2 years (Carpenter et al.,  
40 2014). The global emissions of  $\text{CH}_3\text{Cl}$  have been estimated to be in the range of 4 to 5  $\text{Tg yr}^{-1}$   
41 ( $1 \text{ Tg} = 10^{12} \text{ g}$ ) stemming from predominantly natural but also anthropogenic sources  
42 (Montzka and Fraser, 2003; WMO, 2011; Carpenter et al., 2014). However, current estimates  
43 of the  $\text{CH}_3\text{Cl}$  global budget and the apportionment between sources and sinks are still highly  
44 uncertain. Known natural sources of  $\text{CH}_3\text{Cl}$  include tropical plants (Yokouchi et al., 2002;  
45 Yokouchi et al., 2007; Umezawa et al., 2015), wood-rotting fungi (Harper, 1985), oceans  
46 (Moore et al., 1996), plants of salt marshes (Rhew et al., 2003; Rhew et al., 2000), aerated  
47 and flooded soil (Redeker et al., 2000; Keppler et al., 2000), senescent leaves and leaf litter  
48 (Hamilton et al., 2003; Derendorp et al., 2011) and wild fires. Anthropogenic  $\text{CH}_3\text{Cl}$  release  
49 to the atmosphere comes from the combustion of coal and biomass with minor emissions  
50 from cattle (Williams et al., 1999) and humans (Keppler et al., 2017). In addition, it has been  
51 reported that emissions from industrial sources, particularly in China, might be much higher  
52 than previously assumed (Li et al., 2016).

53 The dominant sink for atmospheric  $\text{CH}_3\text{Cl}$  results from the reaction with photochemically-  
54 produced hydroxyl radicals (OH), currently estimated at about  $2.8 \text{ Tg yr}^{-1}$  (Carpenter et al.,  
55 2014). Furthermore, in the marine boundary layer the reaction of  $\text{CH}_3\text{Cl}$  with chlorine  
56 radicals (Cl) represents another sink estimated to account for up to  $0.4 \text{ Tg yr}^{-1}$  (Khalil et al.,  
57 1999; Montzka and Fraser, 2003). Microbial  $\text{CH}_3\text{Cl}$  degradation in soils may be a relevant  
58 additional global sink (McAnulla et al., 2001; Harper et al., 2003; Miller et al., 2004; Jaeger  
59 et al., 2018a) but its impact on the global  $\text{CH}_3\text{Cl}$  budget is still highly uncertain. The  
60 microbial  $\text{CH}_3\text{Cl}$  soil sink strength has been estimated to range from 0.1 to  $1.6 \text{ Tg yr}^{-1}$   
61 (Harper et al., 2003; Keppler et al., 2005; Carpenter et al., 2014). Moreover, small  
62 proportions of tropospheric  $\text{CH}_3\text{Cl}$  are lost to the stratosphere ( $146 \text{ Gg yr}^{-1}$ ,  $1 \text{ Gg} = 10^9 \text{ g}$ ) and



63 to cold polar oceans ( $370 \text{ Gg yr}^{-1}$ ) though oceans in total are a net source (Carpenter et al.,  
64 2014).

65 A potentially powerful tool in the investigation of the budgets of atmospheric volatile organic  
66 compounds is the use of stable isotope ratios (Brenninkmeijer et al., 2003; Gensch et al.,  
67 2014). Stable isotope analysis, when used in combination with  $\text{CH}_3\text{Cl}$  flux measurements, has  
68 the potential to better constrain the atmospheric  $\text{CH}_3\text{Cl}$  budget as suggested by Keppler et al.  
69 (2005) and Saito & Yokouchi (2008). The isotopic composition of tropospheric  $\text{CH}_3\text{Cl}$   
70 depends on the isotopic source signatures and the kinetic isotope effects (KIE) of the sinks.  
71 Several studies have investigated the stable carbon isotope source signature of  $\text{CH}_3\text{Cl}$   
72 produced via biotic and abiotic processes, however, for a more detailed overview we refer  
73 readers to the studies reported by Keppler et al. (2005) and Saito & Yokouchi (2008).  
74 Moreover, a few studies have measured the KIE of stable carbon isotopes of  $\text{CH}_3\text{Cl}$  during  
75 oxidation or biodegradation by bacterial isolates (Miller et al., 2001; Nadalig et al., 2013;  
76 Nadalig et al., 2014) or in soils under laboratory conditions (Miller et al., 2004; Jaeger et al.,  
77 2018a). The first, and so far, only available analysis of the KIE for reaction of  $\text{CH}_3\text{Cl}$  with  
78 OH has been reported by Gola et al. (2005) and revealed an unexpectedly large stable carbon  
79 isotope fractionation. The experiments were carried out in a smog chamber using long path  
80 Fourier-transform infrared spectroscopy (FTIR) detection. However, in view of the  
81 unexpected isotope fractionation we consider it important to confirm this result using other  
82 measurement methods such as stable isotope ratio mass spectrometry (IRMS).

83 So far isotopic investigations of  $\text{CH}_3\text{Cl}$  have predominantly focused on stable carbon isotope  
84 measurements. Stable hydrogen isotope measurements including both sources and sinks of  
85  $\text{CH}_3\text{Cl}$  have become available only recently (Greule et al., 2012; Nadalig et al., 2014; Nadalig  
86 et al., 2013; Jaeger et al., 2018b; Jaeger et al., 2018a). Moreover, relative rate experiments  
87 have been carried out for three isotopologues of  $\text{CH}_3\text{Cl}$  and their reactions with Cl and OH.  
88 The OH and Cl reaction rates of  $\text{CH}_2\text{DCl}$  were measured by long-path FTIR spectroscopy  
89 relative to  $\text{CH}_3\text{Cl}$  at  $298 \pm 2 \text{ K}$  and 1 atm (Sellevåg et al., 2006) (Table 1).

90 In this manuscript, using a  $3.5 \text{ m}^3$  Teflon smog chamber and IRMS measurements, we  
91 present results from kinetic studies of the hydrogen isotope fractionation in the atmospheric  
92 OH and Cl loss processes of  $\text{CH}_3\text{Cl}$ . Furthermore, we also measured the isotope fractionation  
93 for the reaction between methane ( $\text{CH}_4$ ) and OH using a similar experimental design and  
94 compared this value with those from previous studies.



## 95 2 Materials and Methods

### 96 2.1 Smog chamber experiments with chloromethane

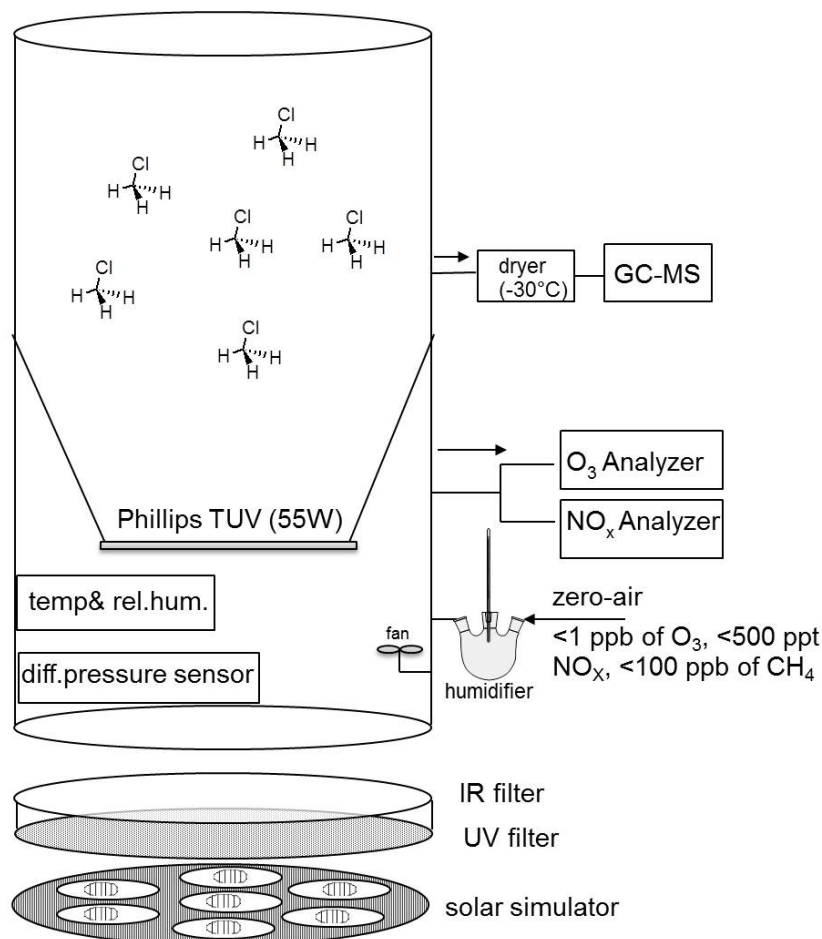
97 The isotope fractionation experiments were performed in a 3.5 m<sup>3</sup> Teflon smog-chamber  
98 (fluorinated ethylene propylene, FEP 200A, DuPont, Wilmington, DE, USA) with initial  
99 CH<sub>3</sub>Cl mixing ratio of about 10 parts per million by volume (ppmv). Atomic chlorine were  
100 generated via photolysis of molecular chlorine (Cl<sub>2</sub>) (Rießner Gase, 0.971% Cl<sub>2</sub> in N<sub>2</sub>) by a  
101 solar simulator with an actinic flux comparable to the sun in mid-summer in Germany  
102 (Bleicher et al., 2014). Hydroxyl radicals were generated via the photolysis of ozone (O<sub>3</sub>) at  
103 253.7 nm in the presence of water vapor (RH = 70%) (produced by double-distilled water in a  
104 three-neck bottle humidifier) and/or H<sub>2</sub>. To obtain efficient OH formation, a Philips TUV  
105 lamp (55 W) was welded in Teflon film (FEP 200) and mounted inside the smog chamber. O<sub>3</sub>  
106 was monitored by a chemiluminescence analyzer (UPK 8001). The chamber was  
107 continuously flushed with purified, hydrocarbon-free zero air (zero-air-generator, cmc  
108 instruments, <1 ppbv of O<sub>3</sub>, <500 pptv NO<sub>x</sub>, <100 ppbv of CH<sub>4</sub>) at a rate of 4 L min<sup>-1</sup> to  
109 maintain a slight overpressure of 0.5-1 Pa logged with a differential pressure sensor  
110 (Kalinsky Elektronik DS1). The quality of the air inside the chamber in terms of possible  
111 contamination was controlled by monitoring NO and NO<sub>x</sub> (EcoPhysics CLD 88p, coupled  
112 with a photolytic converter, EcoPhysics PLC 860). Perfluorohexane (PFH) with an initial  
113 mixing ratio of ~25 parts per billion by volume (ppbv) was used as an internal standard to  
114 correct the resulting concentrations for dilution. The temperature was set to 20±1°C and  
115 monitored, together with the relative humidity, by a Teflon-cased sensor (Rotronic, HC2-  
116 IC102). To guarantee constant mixing and small temperature gradients, a Teflon fan was  
117 mounted and operated inside the chamber. More detailed specification of the smog chamber  
118 can be found elsewhere (e.g. Wittmer et al., 2015). The mixing ratios of CH<sub>3</sub>Cl and PFH  
119 were monitored by gas chromatography-mass spectrometry (GC-MS, Agilent Technologies,  
120 Palo Alto, CA) with a time resolution of 15 minutes throughout the experiments. Aliquots (5  
121 ml) were withdrawn from the chamber with a gas tight syringe, injected into a stream of He  
122 (30 ml min<sup>-1</sup>) and directed to a pre-concentration unit that was attached to the GC-MS. The  
123 pre-concentration unit consisted of a simple 8 port valve (VICI Valco) equipped with two  
124 cryotrap traps made of fused silica, which were immersed in liquid nitrogen for trapping the  
125 analytes. Prior to each sample measurement, a gaseous standard (5 ml of 100 ppmv CH<sub>3</sub>Cl in  
126 N<sub>2</sub>) was measured. Figure 1 shows the design of the smog chamber used in our experiments.



127 In the  $\text{CH}_3\text{Cl}$  and OH experiments (1 and 2) 2000 ppmv  $\text{H}_2$  was used to scavenge chlorine  
128 atoms originating from the photolysis or oxidation of formyl chloride ( $\text{HCOCl}$ ), which forms  
129 as an intermediate in the reaction cascade. Under the experimental conditions typically more  
130 than 70% of the  $\text{CH}_3\text{Cl}$  was degraded within 7 to 10 h. From each experiment ( $\text{CH}_3\text{Cl} + \text{OH}$   
131 and  $\text{CH}_3\text{Cl} + \text{Cl}$ ) 10 to 15 canister samples (2 L stainless steel, evacuated  $<10^{-4}$  mbar) were  
132 collected at regular time intervals for subsequent stable hydrogen isotope measurements at  
133 Heidelberg University.

134

135 **Figure 1:** Scheme of the experimental smog chamber



136

137

138



## 139 2.2 Smog chamber degradation experiments with methane

140 The CH<sub>4</sub> degradation experiments were carried under the same conditions as the CH<sub>3</sub>Cl  
141 degradation experiments but without PFA as an internal standard. Instead we used the  
142 flushing flow rate of zero air to account for the dilution during the experiment. The initial  
143 CH<sub>4</sub> mixing ratio was 6 ppmv. Throughout these experiments CH<sub>4</sub> mixing ratios were  
144 monitored with a Picarro G225i cavity ring down spectrometer directly connected to the  
145 chamber.

146

## 147 2.3 Stable hydrogen isotope analysis using isotope ratio mass spectrometry

### 148 2.3.1 Chloromethane

149 Stable hydrogen isotope ratios of CH<sub>3</sub>Cl were measured by an in-house built cryogenic pre-  
150 concentration unit coupled to a Hewlett Packard HP 6890 gas chromatograph (Agilent  
151 Technologies, Palo Alto, CA) and an isotope ratio mass spectrometer (IRMS) (Isoprime,  
152 Manchester, UK) as described in detail by Greule et al. (2012). Diverging from the method of  
153 Greule et al. (2012) a ceramic tube reactor without chromium pellets at 1450°C was instead  
154 used for high-temperature conversion (HTC). A tank of high-purity H<sub>2</sub> (Alphagaz 2,  
155 hydrogen 6.0, Air Liquide, Düsseldorf, Germany) with a δ<sup>2</sup>H value of ~-250 mUr (milliurey  
156 = 0.001 = 1‰, cf. section below) versus VSMOV was used as the working gas. All measured  
157 sample δ<sup>2</sup>H values were monitored for their relative trueness by analyzing an in-house  
158 working standard of known δ<sup>2</sup>H value. The CH<sub>3</sub>Cl working standard was calibrated against  
159 IAEA standards NBS 22, LVSEC (carbon), VSMOW and SLAP (hydrogen) using TC/EA-  
160 IRMS (elemental analyser-isotopic ratio mass spectrometer, IsoLab, Max Planck Institute for  
161 Biogeochemistry, Jena, Germany) resulting in a δ<sup>2</sup>H value of -140.1 ± 1.0 mUr vs. VSMOW  
162 (n = 10, 1σ). The H<sub>3</sub><sup>+</sup> factor, determined daily during this investigation (two different  
163 measurement periods), was in the range of 5.75 - 6.16 (first period) and 8.90 - 9.21 (second  
164 period). The mean precision based on replicate measurements (n = 6) of the CH<sub>3</sub>Cl working  
165 standard was 2.1 mUr and 3.8 mUr for the first and second measurement periods,  
166 respectively. Samples were analyzed three times (n = 3), and the standard deviations (SD) of  
167 the measurements were in the range of 1.2 to 103.8 mUr. Lowest SD were observed for  
168 samples with lowest δ<sup>2</sup>H values (~-140 mUr) and highest mixing ratios and higher SD for  
169 samples with highest δ<sup>2</sup>H values (~+800 mUr) and lowest mixing ratios.



170 To comply with International System of Units (SI) guidelines, we follow the proposal of  
171 Brand and Coplen (2012) and use the symbol Ur, after H.C. Urey (Urey, 1948), as the isotope  
172 delta (Coplen, 2011) value unit. Thus, an isotope-delta value expressed traditionally as  $-50$   
173 ‰ can be written  $-50$  mUr. Similarly as for the  $\delta^2\text{H}$  values, throughout the manuscript we  
174 also report the isotope enrichment factor  $\epsilon$  in mUr.

175 Please note that the above described 1-point calibration of the  $\delta^2\text{H}$  data might be affected by  
176 an additional error ("scale compression") and particularly might affect the uncertainties of the  
177 very positive  $\delta^2\text{H}$  values. Unfortunately  $\text{CH}_3\text{Cl}$  working standards with distinct isotopic  
178 signatures spanning the full range of measured  $\delta^2\text{H}$  values ( $-150$  to  $\sim+800$  mUr) are not  
179 currently available to eliminate or minimize such an error.

180

### 181 **2.3.2 Methane**

182 Stable hydrogen isotope ratios of  $\text{CH}_4$  were analyzed using an in-house built cryogenic pre-  
183 concentration unit coupled to a Hewlett Packard HP 6890 gas chromatograph (Agilent  
184 Technologies, Palo Alto, CA) and an isotope ratio mass spectrometer (DeltaPlus XL,  
185 ThermoQuest Finnigan, Bremen, Germany). The working gas was the same as that used for  
186  $\delta^2\text{H}$  analysis of  $\text{CH}_3\text{Cl}$  (c.f. section 2.3.1.).

187 All  $\delta^2\text{H}$  values obtained from analysis of  $\text{CH}_4$  were corrected using two  $\text{CH}_4$  working  
188 standards (isometric instruments, Victoria, Canada) calibrated against IAEA and NIST  
189 reference substances (not specified by the company). The calibrated  $\delta^2\text{H}$  values of the  
190 working standard in mUr vs. V-SMOW were  $-144 \pm 4$  mUr and  $-138 \pm 4$  mUr.

191 The  $\text{H}_3^+$  factor determined daily during the two week measurement period was in the range  
192 2.38–2.43. The daily average precision based on replicate measurements of the  $\text{CH}_4$  working  
193 standard was 4.9 mUr ( $n = 7$ ). Samples were analyzed 3 times ( $n = 3$ ), and the SD of the  
194 measurements were in the range of 1.4 to 40.9 mUr. Lowest SD were observed for samples  
195 with lowest  $\delta^2\text{H}$  values ( $\sim-140$  mUr) and highest mixing ratios and higher SD for samples  
196 with highest  $\delta^2\text{H}$  values ( $\sim+800$  mUr) and lowest mixing ratios.

197

198

199

200



201 **2.4 Kinetic isotope effect, fractionation constant  $\alpha$  and the isotope enrichment constant  $\epsilon$**

202 The isotopic composition of atmospheric compounds might be altered by the kinetic isotope  
 203 effects of physical, chemical or biological loss processes. The kinetic isotope effect (KIE) is  
 204 usually defined as:

$$205 \quad KIE = \frac{k_1}{k_2} \quad (1)$$

206 where  $k_1$  and  $k_2$  are the reaction rate constants for loss of the lighter and the heavier  
 207 isotopologues, respectively. The KIE is typically expressed as isotope fractionation  $\epsilon$  (also  
 208 termed isotope enrichment constant) or isotope fractionation constant  $\alpha$ .

209 In this study the isotope fractionation constant  $\alpha$  and the isotope enrichment constant  $\epsilon$  are  
 210 derived from the slope of the Rayleigh plot according to (Clark and Fritz, 1997; Elsner et al.,  
 211 2005) and equation 2:

$$213 \quad \ln \frac{R_t}{R_0} = \ln \left( \frac{\delta^2 H_t + 1000}{\delta^2 H_0 + 1000} \right) = \ln \frac{(\delta^2 H_0 + \Delta \delta^2 H + 1)}{(\delta^2 H_0 + 1)} \cong (\alpha - 1) \cdot \ln f = \epsilon \cdot \ln f \quad (2)$$

214

215 Where  $R_t$  and  $R_0$  are the  $^2\text{H}/^1\text{H}$  ratios in  $\text{CH}_3\text{Cl}$  or  $\text{CH}_4$  at the different time points and time  
 216 zero, respectively, and  $f$  is the remaining  $\text{CH}_3\text{Cl}$  or  $\text{CH}_4$  fraction at the different time points.  
 217 Negative values of  $\epsilon$  indicates that the remaining  $\text{CH}_3\text{Cl}$  or  $\text{CH}_4$  is enriched in the heavier  
 218 isotope and corresponds to a  $\alpha < 1$ , meaning that over the entire experiment, the heavier  $\text{CH}_3\text{Cl}$   
 219 or  $\text{CH}_4$  react by this factor more slowly than the lighter  $\text{CH}_3\text{Cl}$  or  $\text{CH}_4$ .

220 The kinetic isotope effect is then calculated as:

$$221 \quad KIE = \frac{1}{\alpha} \quad (3)$$

222 To correct for ongoing analyte dilution the remaining fraction  $f$  has been calculated as  
 223 follows

$$224 \quad f = c_{xT} \cdot c_{i0} / (c_{x0} \cdot c_{iT}) \quad (4)$$

225 where  $c_{x0}$  and  $c_{xT}$  are the mixing ratios of  $\text{CH}_3\text{Cl}$  at time zero and time  $t$  and  $c_{i0}$  and  $c_{iT}$  are  
 226 the respective concentrations of the internal standard PFH.



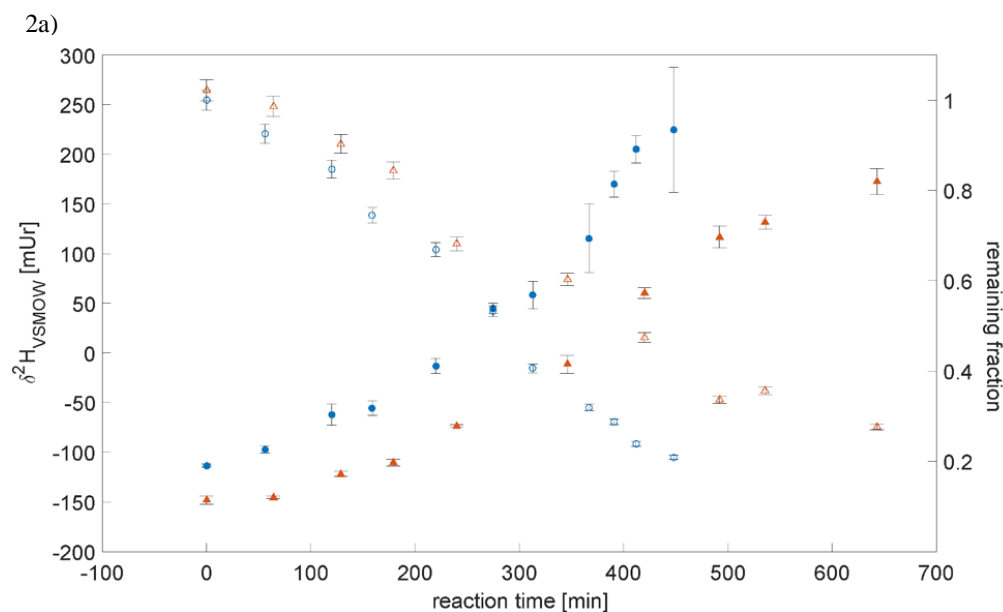


### 227 3 Results

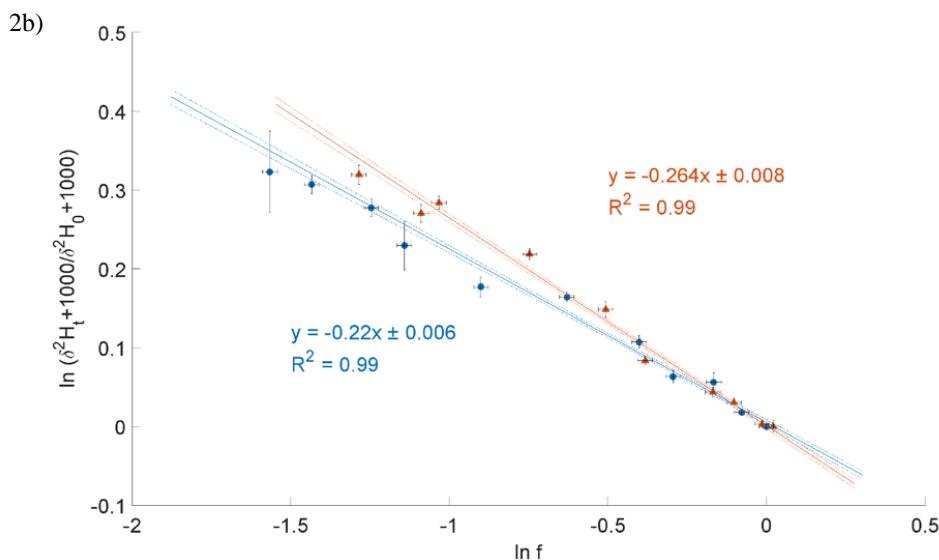
228 The first experiment of CH<sub>3</sub>Cl degradation with OH was performed on the 25/02/2014 and  
229 repeated under similar conditions on the 03/02/2015. Under the experimental conditions (see  
230 methods section) more than 70% of the CH<sub>3</sub>Cl was degraded within 7 to 10 h. The results  
231 from these two experiments are shown in Figure 2. Both the trend of changes in δ<sup>2</sup>H values of  
232 CH<sub>3</sub>Cl as well as the remaining fraction of CH<sub>3</sub>Cl observed in the two independent  
233 experiments are in good agreement (Figure 2a). The calculated ε values for experiments 1 and  
234 2 are -264 ± 8 mUr and -220 ± 6 mUr, respectively (Figure 2b), with a correlation coefficient  
235 R<sup>2</sup> of the slope of the regression line of 0.99 for both experiments.

236 **Figure 2:** Reaction of CH<sub>3</sub>Cl and OH. Two independent experiments (triangles and dots)  
237 were carried out using an initial mixing ratio of ~10 ppmv CH<sub>3</sub>Cl. More than 70% of the  
238 CH<sub>3</sub>Cl was degraded within 8 to 10 h. (a) Measured δ<sup>2</sup>H values (filled circles and triangles)  
239 of CH<sub>3</sub>Cl versus residual fraction (open circles and triangles) of CH<sub>3</sub>Cl (calculated from  
240 changes of CH<sub>3</sub>Cl and PFH). Error bars of δ<sup>2</sup>H value of CH<sub>3</sub>Cl indicate the standard  
241 deviation (SD) of the mean of three replicate measurements. Some error bars lie within the  
242 symbol. (b) Rayleigh plot (equation 2). Error bars were calculated by error propagation  
243 including uncertainties in δ<sup>2</sup>H values of CH<sub>3</sub>Cl and the remaining fraction. Dashed lines  
244 represent 95% confidence intervals of the linear regressions (bold lines).

245



246



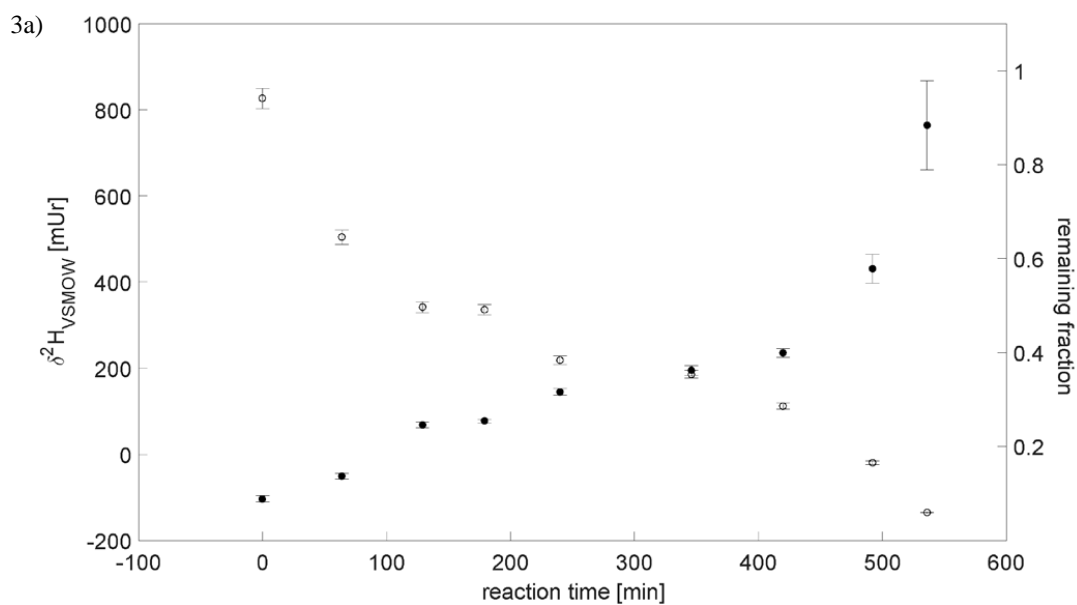
247

248

249 The  $\text{CH}_3\text{Cl}$  degradation with Cl experiment was conducted on the 18/02/2014. Here, over  
250 90% of  $\text{CH}_3\text{Cl}$  was degraded during reaction with Cl radicals within 7 to 8 hours (Figure 3a).  
251 The calculated  $\epsilon$  of experiment 3 is  $-280 \pm 11$  mUr (Figure 3b) with a correlation coefficient  
252 of the slope of the regression line of 0.99. Due to limited analytical resources it was not  
253 possible to repeat this experiment.

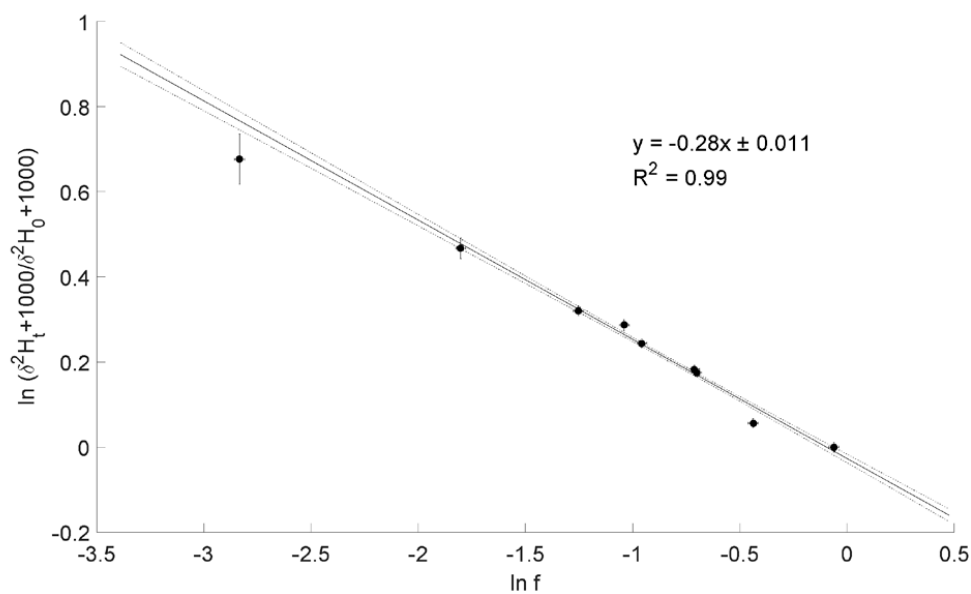
254

255 **Figure 3:** Reaction of  $\text{CH}_3\text{Cl}$  and Cl. Initial mixing ratio of  $\text{CH}_3\text{Cl}$  was  $\sim 10$  ppmv. More than  
256 90% of the  $\text{CH}_3\text{Cl}$  was degraded within 7 to 8 h. (a) Measured  $\delta^2\text{H}$  values (filled circles) of  
257  $\text{CH}_3\text{Cl}$  versus residual fraction (open diamonds)  $\text{CH}_3\text{Cl}$ . Error bars of  $\delta^2\text{H}$  values of  $\text{CH}_3\text{Cl}$   
258 indicate the standard deviation (SD) of the mean of three replicate measurements. Some error  
259 bars lie within the symbol. (b) Rayleigh plot (equation 2). Data are expressed as the  
260 mean  $\pm$  standard error of the mean,  $n = 3$ . Error bars were calculated by error propagation  
261 including uncertainties in  $\delta^2\text{H}$  values of  $\text{CH}_3\text{Cl}$ . Dashed lines represent 95% confidence  
262 intervals of the linear regressions (bold line).



263

264 3b)



265

266

267

268 The experiment to determine the isotope enrichment constant of the degradation of  $\text{CH}_4$  by  
269 hydroxyl radicals was conducted on the 02/02/2015. Over 80% of  $\text{CH}_4$  was degraded during



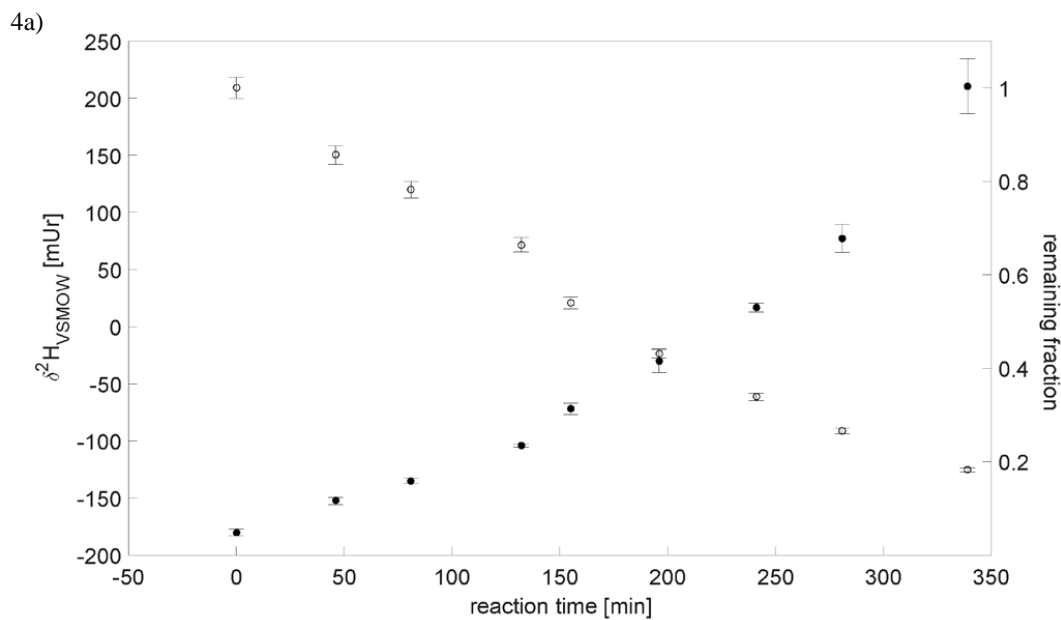
270 reaction with OH radicals within 7 hours (Figure 4a). The calculated  $\epsilon$  of experiment 4 is -  
271  $205 \pm 6$  mUr (Figure 4b) with a correlation coefficient of the slope of the regression line of  
272 0.99.

273

274

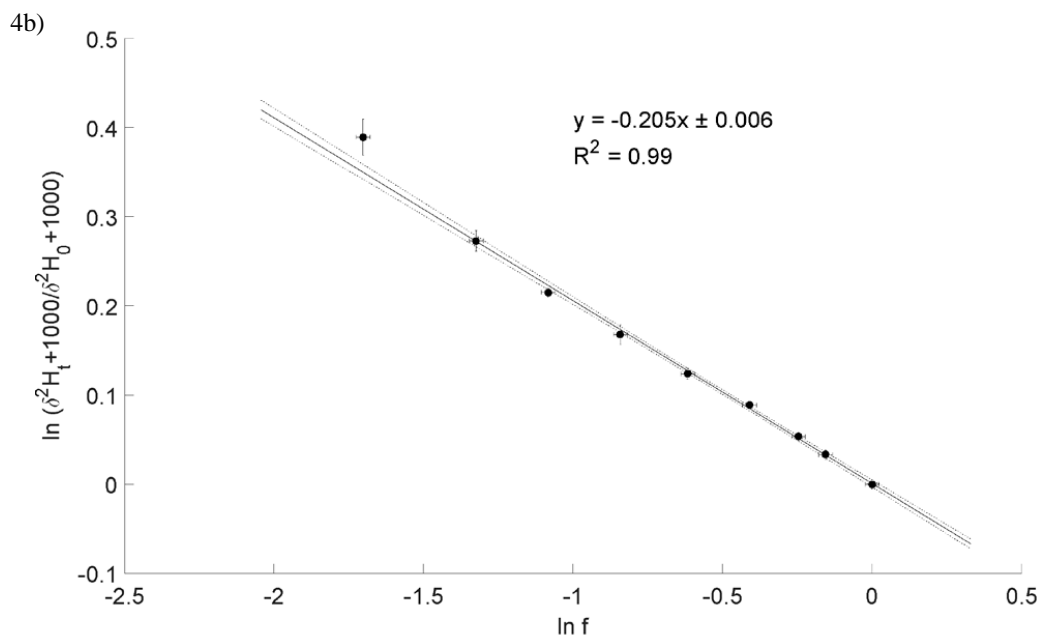
275 **Figure 4:** Reaction of CH<sub>4</sub> and OH. Initial mixing ratio of CH<sub>4</sub> was ~6 ppmv. More than 80%  
276 of the CH<sub>4</sub> was degraded within 7 h. (a) Measured  $\delta^2\text{H}$  values of CH<sub>4</sub> versus residual fraction  
277 of CH<sub>4</sub>. Error bars of  $\delta^2\text{H}$  values of CH<sub>4</sub> indicate the standard deviation (SD) of the mean of  
278 three replicate measurements. Some error bars lie within the symbol. (b) Rayleigh plot  
279 (equation 2). Error bars were calculated by error propagation including uncertainties in  $\delta^2\text{H}$   
280 values of CH<sub>4</sub> and the remaining fraction. Dashed lines represent 95% confidence intervals of  
281 the linear regressions (bold line).

282



283

284



285

#### 286 4 Discussion

287 Chloromethane reacts with both hydroxyl and chlorine radicals in the atmosphere. The first  
288 degradation step of  $\text{CH}_3\text{Cl}$  in both reactions is the abstraction of a hydrogen atom to yield  
289  $\text{CH}_2\text{Cl}$  and  $\text{H}_2\text{O}$  or  $\text{HCl}$ , respectively (Spence et al., 1976; Khalil and Rasmussen, 1999). In  
290 both reactions hydrogen is directly present in the reacting bond, and thus influenced by the  
291 so-called primary isotope effect (Elsner et al., 2005). Particularly for hydrogen these primary  
292 kinetic isotope effects are in general large as they involve a large change in relative mass of  
293 the atoms being abstracted. In the following we would like to discuss and compare our results  
294 with (i) previous work conducted by (Sellevåg et al., 2006), (ii) with OH degradation  
295 experiments of  $\text{CH}_4$  and (iii) with the very recent report of biochemical degradation of  $\text{CH}_3\text{Cl}$   
296 in soils and plants (Jaeger et al., 2018b; Jaeger et al., 2018a).

297 Although our experimental results show relatively large hydrogen isotope fractionations with  
298  $\epsilon$  values of -242 (mean result from two independent experiments) and -280 mUr, for reaction  
299 of  $\text{CH}_3\text{Cl}$  with OH and Cl radicals, respectively, they are smaller than the isotope  
300 fractionations previously measured and theoretically calculated by (Sellevåg et al., 2006)  
301 (Table 1). These researchers employed smog chamber experiments at 298 K and used FTIR  
302 measurements to determine the stable hydrogen isotope fractionation of  $\text{CH}_3\text{Cl}$  and reported  $\epsilon$   
303 values of -410 and -420 mUr for the reaction of  $\text{CH}_3\text{Cl}$  with OH and Cl radicals, respectively.



304 They also performed theoretical calculations of  $\epsilon$  for the reactions of  $\text{CH}_2\text{DCI}$  with OH and  
305 Cl radicals and reported  $\epsilon$  values in the range of -330 to -430 and -540 to -590 mUr,  
306 respectively (Table 1). Whilst we do not know the reasons for the large discrepancies in the  
307 experimental  $\epsilon$  values observed here and those reported by Sellevåg et al. (2006), we suggest  
308 that they may be due to differences in the experimental smog chamber set-up or the different  
309 measurement techniques employed in each of the studies. However, we also conducted  
310 similar smog chamber experiments for the degradation of  $\text{CH}_4$  with hydroxyl radicals (see  
311 methods section and Figure 4) and calculated an  $\epsilon$  value of  $-205 \pm 6$  mUr for the reaction of  
312  $\text{CH}_4$  with OH radicals at a temperature of  $293 \pm 1$  K. In Table 1 we compare our results with  
313 those from a number of previous studies (Saueressig et al., 2001; Sellevåg et al., 2006;  
314 DeMore, 1993; Gierczak et al., 1997; Xiao et al., 1993), which were conducted at  
315 temperatures ranging from 277 to 298 K (Table 1). The  $\epsilon$  values for the reaction of  $\text{CH}_4$  with  
316 OH radicals from all studies ranged from -145 to -294 mUr with a mean value of  $-229 \pm 44$   
317 mUr with the most negative  $\epsilon$  value of  $-294 \pm 18$  mUr reported by Sellavag and coworkers  
318 (2006). The  $\epsilon$  value found in this study ( $-205 \pm 6$  mUr) was in good agreement with previous  
319 experimentally reported values conducted at similar temperatures. This finding gave us  
320 confidence that our experimental design and the measurements made using GC-IRMS were  
321 reliable.

322 Compared to primary isotope effects, changes in bonding are much smaller in the case of  
323 secondary isotope effects, where positions adjacent to the reacting bond are only slightly  
324 affected by the proximity to the reaction centre (Elsner et al., 2005; Kirsch, 1977). It was  
325 suggested that for the same element, secondary isotope effects are generally at least 1 order of  
326 magnitude smaller than primary isotope effects (Kirsch, 1977; Westaway, 1987; Merrigan et  
327 al., 1999).

328 We therefore compared our results from chemical degradation experiments with those from  
329 recently reported biochemical degradation experiments (Jaeger et al., 2018a; Jaeger et al.,  
330 2018b). So far, the only known pathway for biochemical consumption of  $\text{CH}_3\text{Cl}$  is corrinoid-  
331 and tetrahydrofolate-dependent and is termed cmu (abbreviation for chloromethane  
332 utilization). This pathway was characterized in detail for the aerobic facultative  
333 methylotrophic strain *Methylobacterium extorquens* CM4 (Vannelli et al., 1999) and involves  
334 genes that were also detected in several other chloromethane-degrading strains (Schafer et al.,  
335 2007; Nadalig et al., 2013; Nadalig et al., 2011). During degradation of  $\text{CH}_3\text{Cl}$  the methyl  
336 group is transferred to a corrinoid cofactor by the protein CmuA. In this case the carbon-



337 chlorine bond of  $\text{CH}_3\text{Cl}$  is broken and thus since the hydrogen atoms are adjacent to the  
338 reacting bond only a secondary isotope effect would be expected. Indeed, the first  $\epsilon$  values  
339 reported (Jaeger et al., 2018a; Jaeger et al., 2018b) for  $\text{CH}_3\text{Cl}$  biodegradation by different  
340 soils and plants (ferns) are in the range of  $-50 \pm 13$  mUr and  $-8 \pm 19$  mUr, respectively, and  
341 thus showing considerably smaller kinetic isotope effects than for chemical degradation of  
342  $\text{CH}_3\text{Cl}$  by OH and Cl radicals measured in either this study or reported by Sellevåg et al.  
343 (2006).

344

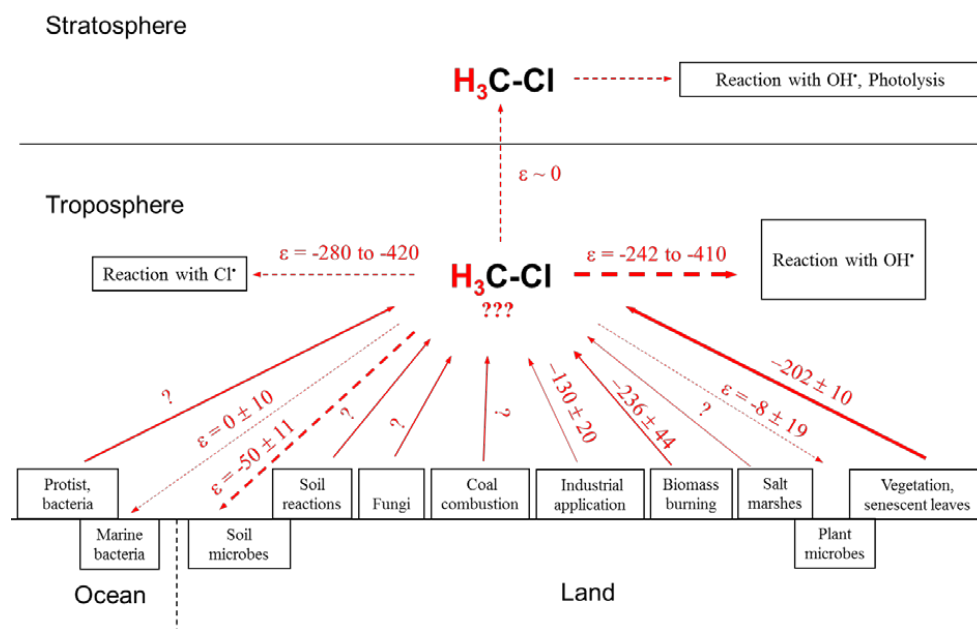
## 345 **5 Conclusions and future perspectives**

346 We have performed experiments to measure the hydrogen isotope fractionation of the  
347 remaining unreacted  $\text{CH}_3\text{Cl}$  following its degradation by hydroxyl and chlorine radicals in a  
348  $3.5 \text{ m}^3$  Teflon smog-chamber at  $293 \pm 1 \text{ K}$ .  $\delta^2\text{H}$  values of  $\text{CH}_3\text{Cl}$  were measured using GC-  
349 IRMS. The calculated isotope fractionations of  $\text{CH}_3\text{Cl}$  for the reactions with hydroxyl and  
350 with chlorine radicals were found to be smaller than either the experimentally measured (by  
351 FTIR) or theoretical values reported by Sellevåg et al. (2006). We also performed  
352 degradation experiments of  $\text{CH}_4$  using the same smog-chamber facilities yielding an isotope  
353 enrichment constant for the reaction of  $\text{CH}_4$  with hydroxyl radicals of  $-205 \pm 6$  mUr which is  
354 in excellent agreement with previous reported results. Although stable hydrogen isotope  
355 measurements of  $\text{CH}_3\text{Cl}$  sources are still scarce, some recent studies have reported first data  
356 on  $\delta^2\text{H}$  values of  $\text{CH}_3\text{Cl}$  sources and  $\epsilon$  values on sinks (Greule et al., 2012; Jaeger et al.,  
357 2018a; Jaeger et al., 2018b; Nadalig et al., 2014; Nadalig et al., 2013).

358 We have summarized all available information regarding  $\delta^2\text{H}$  values of environmental  $\text{CH}_3\text{Cl}$   
359 sources in Table 2. Furthermore, the known  $\text{CH}_3\text{Cl}$  sinks and their associated isotope  
360 enrichment constants are presented in Table 3. Eventually Figure 5 displays the global  $\text{CH}_3\text{Cl}$   
361 budget showing the known hydrogen isotope signatures of sources and isotope enrichment  
362 constants associated with sinks.

363 **Figure 5.** Scheme of major sources and sinks involved in the global  $\text{CH}_3\text{Cl}$  cycle (modified  
364 after Keppler et al., 2005) with known (experimentally determined) corresponding  $\delta^2\text{H}$  values  
365 and isotope enrichment constants, respectively. Red straight and dashed lines of arrows  
366 indicate sources and sinks of  $\text{CH}_3\text{Cl}$ , respectively. Question marks indicate where currently  
367 no data exist. All values are given in mUr.

368



369  
 370

371 Our results suggest that stable hydrogen isotope measurements of both sources and sinks of  
 372  $\text{CH}_3\text{Cl}$  and particularly the observed large kinetic isotope effect of the atmospheric  $\text{CH}_3\text{Cl}$   
 373 sinks might strongly assist with the refinement of current models of the global atmospheric  
 374  $\text{CH}_3\text{Cl}$  budget. In contrast to the large hydrogen fractionation of  $\text{CH}_3\text{Cl}$  by chemical  
 375 degradation of OH and Cl radicals, the isotope fractionation of  $\text{CH}_3\text{Cl}$  biodegradation are in  
 376 the range of an order of magnitude lower. This therefore holds the opportunity to improve our  
 377 understanding of the global  $\text{CH}_3\text{Cl}$  budget once the  $\delta^2\text{H}$  value of atmospheric  $\text{CH}_3\text{Cl}$  has been  
 378 measured. The stable hydrogen isotopic composition of tropospheric  $\text{CH}_3\text{Cl}$  depends on the  
 379 isotopic source signatures and the kinetic isotope effects of the sinks, primarily the reaction  
 380 with OH and consumption by soils and potentially plants.

381 Several attempts at modelling the global  $\text{CH}_3\text{Cl}$  budget using stable carbon isotope ratios  
 382 have already been made (Harper et al., 2001; Harper et al., 2003; Thompson et al., 2002;  
 383 Keppler et al., 2005; Saito and Yokouchi, 2008) but there are still major uncertainties  
 384 regarding source and sink strengths as well as the respective stable isotope signatures.  
 385 Therefore, we now suggest combining our knowledge of stable carbon and hydrogen isotopes  
 386 of  $\text{CH}_3\text{Cl}$  in the environment. Such a two dimensional (2D) stable isotope approach of  
 387 hydrogen and carbon can be used to better understand the processes of  $\text{CH}_3\text{Cl}$  biodegradation  
 388 and formation. Furthermore, when this approach is combined with  $\text{CH}_3\text{Cl}$  flux estimates it





389 could help to better constrain the strength of CH<sub>3</sub>Cl sinks and sources within the global  
390 CH<sub>3</sub>Cl budget (Nadalig et al., 2014; Jaeger et al. 2018b)

391 We would highlight that currently no data is available for the  $\delta^2\text{H}$  value of atmospheric  
392 CH<sub>3</sub>Cl. Although it will be a massive analytical challenge to obtain this value, we strongly  
393 consider that it would likely lead to a better refined isotopic mass balance for atmospheric  
394 CH<sub>3</sub>Cl and thus to our better understanding of the global CH<sub>3</sub>Cl budget.

395

### 396 Acknowledgements

397 This study was supported by DFG (KE 884/8-1; KE 884/8-2, KE 884/10-1) and by the DFG  
398 research unit 763 ‘Natural Halogenation Processes in the Environment - Atmosphere and  
399 Soil’ (KE 884/7-1, SCHO 286/7-2, ZE 792/5-2). We further acknowledge the German  
400 Federal Ministry of Education and Research (BMBF) for funding within SOPRAN ‘Surface  
401 Ocean Processes in the Anthropocene (grants 03F0611E and 03F0662E). We thank John  
402 Hamilton and Carl Brenninkmeijer for comments on an earlier version of the manuscript and  
403 Daniela Polag for statistical evaluation of the data.

404

### 405 References

- 406 Bleicher, S., Buxmann, J. C., Sander, R., Riedel, T. P., Thornton, J. A., Platt, U., and Zetzsch, C.: The  
407 influence of nitrogen oxides on the activation of bromide and chloride in salt aerosol, Atmos. Chem.  
408 Phys. Discuss., 2014, 10135-10166, [10.5194/acpd-14-10135-2014](https://doi.org/10.5194/acpd-14-10135-2014), 2014.
- 409 Brand, W. A., and Coplen, T. B.: Stable isotope deltas: tiny, yet robust signatures in nature, Isot.  
410 Environ. Health Stud., 48, 393-409, [10.1080/10256016.2012.666977](https://doi.org/10.1080/10256016.2012.666977), 2012.
- 411 Brenninkmeijer, C. A. M., Janssen, C., Kaiser, J., Röckmann, T., Rhee, T. S., and Assonov, S. S.:  
412 Isotope Effects in the Chemistry of Atmospheric Trace Compounds, Chem. Rev., 103, 5125-5162,  
413 [10.1021/cr020644k](https://doi.org/10.1021/cr020644k), 2003.
- 414 Carpenter, L. J., Reimann, S., Burkholder, J. B., Clerbaux, C., Hall, B., Hossaini, R., Laube, J., and  
415 Yvon-Lewis, S.: Chapter 1: Update on Ozone-Depleting Substances (ODSs) and Other Gases of  
416 Interest to the Montreal Protocol, in: Scientific Assessment of Ozone Depletion, Global Ozone  
417 Research and Monitoring Project Report, World Meteorological Organization (WMO), 21-125, 2014.
- 418 Clark, I., and Fritz, P.: Environmental isotopes in hydrogeology, Lewis Publishers, New York, 328  
419 pp., 1997.
- 420 Coplen, T. B.: Guidelines and recommended terms for expression of stable-isotope-ratio and gas-ratio  
421 measurement results, Rapid Communications in Mass Spectrometry, 25, 2538-2560,  
422 [10.1002/rcm.5129](https://doi.org/10.1002/rcm.5129), 2011.
- 423 DeMore, W. B.: Rate constant ratio for the reaction of OH with CH<sub>3</sub>D and CH<sub>4</sub>, J. Phys. Chem., 97,  
424 8564-8566, 1993.



- 425 Derendorp, L., Holzinger, R., Wishkerman, A., Keppler, F., and Rockmann, T.: Methyl chloride and  
426 C(2)-C(5) hydrocarbon emissions from dry leaf litter and their dependence on temperature, *Atmos.*  
427 *Environ.*, 45, 3112-3119, [10.1016/j.atmosenv.2011.03.016](https://doi.org/10.1016/j.atmosenv.2011.03.016), 2011.
- 428 Elsner, M., Zwank, L., Hunkeler, D., and Schwarzenbach, R. P.: A new concept linking observable  
429 stable isotope fractionation to transformation pathways of organic pollutants, *Environ Sci Technol.*,  
430 39, 6896-6916, 2005.
- 431 Gensch, I., Kiendler-Scharr, A., and Rudolph, J.: Isotope ratio studies of atmospheric organic  
432 compounds: Principles, methods, applications and potential, *International Journal of Mass*  
433 *Spectrometry*, 365-366, 206-221, <https://doi.org/10.1016/j.ijms.2014.02.004>, 2014.
- 434 Gierczak, T., Talukdar, R. K., Herndon, S. C., Vaghjiani, G. L., and Ravishankara, A. R.: Rate  
435 Coefficients for the Reactions of Hydroxyl Radicals with Methane and Deuterated Methanes, *The*  
436 *Journal of Physical Chemistry A*, 101, 3125-3134, [10.1021/jp963892r](https://doi.org/10.1021/jp963892r), 1997.
- 437 Gola, A. A., D'Anna, B., Feilberg, K. L., Sellevag, S. R., Bache-Andreassen, L., and Nielsen, C. J.:  
438 Kinetic isotope effects in the gas phase reactions of OH and Cl with CH<sub>3</sub>Cl, CD<sub>3</sub>Cl, and (CH<sub>3</sub>Cl)-C-  
439 13, *Atmos. Chem. Phys.*, 5, 2395-2402, 2005.
- 440 Greule, M., Huber, S. G., and Keppler, F.: Stable hydrogen-isotope analysis of methyl chloride  
441 emitted from heated halophytic plants, *Atmos. Environ.*, 62, 584-592,  
442 [10.1016/j.atmosenv.2012.09.007](https://doi.org/10.1016/j.atmosenv.2012.09.007), 2012.
- 443 Hamilton, J. T. G., McRoberts, W. C., Keppler, F., Kalin, R. M., and Harper, D. B.: Chloride  
444 methylation by plant pectin: An efficient environmentally significant process, *Science*, 301, 206-209,  
445 2003.
- 446 Harper, D. B.: Halomethane from halide ion – a highly efficient fungal conversion of environmental  
447 significance, *Nature*, 315, 55-57, 1985.
- 448 Harper, D. B., Kalin, R. M., Hamilton, J. T. G., and Lamb, C.: Carbon isotope ratios for  
449 chloromethane of biological origin: Potential tool in determining biological emissions, *Environ. Sci.*  
450 *Technol.*, 35, 3616-3619, 2001.
- 451 Harper, D. B., Hamilton, J. T. G., Ducrocq, V., Kennedy, J. T., Downey, A., and Kalin, R. M.: The  
452 distinctive isotopic signature of plant-derived chloromethane: possible application in constraining the  
453 atmospheric chloromethane budget, *Chemosphere*, 52, 433-436, 2003.
- 454 Jaeger, N., Besaury, I., Kröber, E., Delort, A.-M., Greule, M., Lenhart, K., Nadalig, T., Vuilleumier,  
455 S., Amato, P., Kolb, S., Bringel, F., and Keppler, F.: Chloromethane degradation in soils - a combined  
456 microbial and two-dimensional stable isotope approach, *Journal of Environmental Quality*, in review,  
457 2018a.
- 458 Jaeger, N., Besaury, L., Röhling, A. N., Koch, F., Delort, A. M., Gasc, C., Greule, M., Kolb, S.,  
459 Nadalig, T., Peyret, P., Vuilleumier, S., Amato, P., Bringel, F., and Keppler, F.: Chloromethane  
460 formation and degradation in the fern phyllosphere, *Science of The Total Environment*, in review,  
461 2018b.
- 462 Keppler, F., Eiden, R., Niedan, V., Pracht, J., and Scholer, H. F.: Halocarbons produced by natural  
463 oxidation processes during degradation of organic matter, *Nature*, 403, 298-301, 2000.
- 464 Keppler, F., Harper, D. B., Rockmann, T., Moore, R. M., and Hamilton, J. T. G.: New insight into the  
465 atmospheric chloromethane budget gained using stable carbon isotope ratios, *Atmos. Chem. Phys.*, 5,  
466 2403-2411, 2005.
- 467 Keppler, F., Fischer, J., Sattler, T., Polag, D., Jaeger, N., Schöler, H. F., and Greule, M.:  
468 Chloromethane emissions in human breath, *Science of The Total Environment*, 605-606, 405-410,  
469 <https://doi.org/10.1016/j.scitotenv.2017.06.202>, 2017.
- 470 Khalil, M. A. K., Moore, R. M., Harper, D. B., Lobert, J. M., Erickson, D. J., Koropalov, V., Sturges,  
471 W. T., and Keene, W. C.: Natural emissions of chlorine-containing gases: Reactive Chlorine  
472 Emissions Inventory, *J. Geophys. Res.-Atmos.*, 104, 8333-8346, 1999.



- 473 Khalil, M. A. K., and Rasmussen, R. A.: Atmospheric methyl chloride, *Atmos. Environ.*, 33, 1305-  
474 1321, [https://doi.org/10.1016/S1352-2310\(98\)00234-9](https://doi.org/10.1016/S1352-2310(98)00234-9), 1999.
- 475 Kirsch, J. F.: in: *Isotope effects on enzyme-catalyzed reactions*, edited by: Cleland, W. W., O'Leary,  
476 M. H., and Northrop, D. B., University Park Press, Baltimore, London, Tokyo, 100-121, 1977.
- 477 Li, S., Park, M.-K., Jo, C. O., and Park, S.: Emission estimates of methyl chloride from industrial  
478 sources in China based on high frequency atmospheric observations, *Journal of Atmospheric*  
479 *Chemistry*, 1-17, 10.1007/s10874-016-9354-4, 2016.
- 480 McAnulla, C., McDonald, I. R., and Murrell, J. C.: Methyl chloride utilising bacteria are ubiquitous in  
481 the natural environment, *FEMS Microbiology Letters*, 201, 151-155, 10.1111/j.1574-  
482 6968.2001.tb10749.x, 2001.
- 483 Merrigan, S. R., Le Gloahec, V. N., Smith, J. A., Barton, D. H. R., and Singleton, D. A.: Separation of  
484 the primary and secondary kinetic isotope effects at a reactive center using starting material  
485 reactivities. Application to the FeCl<sub>3</sub>-Catalyzed oxidation of C-H bonds with tert-butyl  
486 hydroperoxide, *Tetrahedron Letters*, 40, 3847-3850, [https://doi.org/10.1016/S0040-4039\(99\)00637-1](https://doi.org/10.1016/S0040-4039(99)00637-1),  
487 1999.
- 488 Miller, L. G., Kalin, R. M., McCauley, S. E., Hamilton, J. T. G., Harper, D. B., Millet, D. B.,  
489 Oremland, R. S., and Goldstein, A. H.: Large carbon isotope fractionation associated with oxidation  
490 of methyl halides by methylotrophic bacteria, *Proc. Natl. Acad. Sci. U. S. A.*, 98, 5833-5837, 2001.
- 491 Miller, L. G., Warner, K. L., Baesman, S. M., Oremland, R. S., McDonald, I. R., Radajewski, S., and  
492 Murrell, J. C.: Degradation of methyl bromide and methyl chloride in soil microcosms: Use of stable  
493 C isotope fractionation and stable isotope probing to identify reactions and the responsible  
494 microorganisms, *Geochim. Cosmochim. Acta*, 68, 3271-3283, 2004.
- 495 Montzka, S. A., and Fraser, P.: Controlled substances and other source gases, Chapter 1 in *Scientific*  
496 *Assessment of Ozone Depletion: 2002*, World Meteorological Organization, Geneva, 2003.
- 497 Moore, R. M., Groszko, W., and Niven, S. J.: Ocean-atmosphere exchange of methyl chloride:  
498 Results from NW Atlantic and Pacific Ocean studies, *J. Geophys. Res.-Oceans*, 101, 28529-28538,  
499 10.1029/96jc02915, 1996.
- 500 Nadalig, T., Farhan Ul Haque, M., Roselli, S., Schaller, H., Bringel, F., and Vuilleumier, S.: Detection  
501 and isolation of chloromethane-degrading bacteria from the *Arabidopsis thaliana* phyllosphere, and  
502 characterization of chloromethane utilization genes, *FEMS Microbiology Ecology*, 77, 438-448,  
503 10.1111/j.1574-6941.2011.01125.x, 2011.
- 504 Nadalig, T., Greule, M., Bringel, F., Vuilleumier, S., and Keppler, F.: Hydrogen and carbon isotope  
505 fractionation during degradation of chloromethane by methylotrophic bacteria, *MicrobiologyOpen*, 2,  
506 893-900, 10.1002/mbo3.124, 2013.
- 507 Nadalig, T., Greule, M., Bringel, F., Keppler, F., and Vuilleumier, S.: Probing the diversity of  
508 chloromethane-degrading bacteria by comparative genomics and isotopic fractionation, *Frontiers in*  
509 *Microbiology*, 5, 523, 10.3389/fmicb.2014.00523, 2014.
- 510 Redeker, K. R., Wang, N.-Y., Low, J. C., McMillan, A., Tyler, S. C., and Cicerone, R. J.: Emissions  
511 of Methyl Halides and Methane from Rice Paddies, *Science*, 290, 966-969,  
512 10.1126/science.290.5493.966, 2000.
- 513 Rhew, R. C., Miller, B. R., and Weiss, R. F.: Natural methyl bromide and methyl chloride emissions  
514 from coastal salt marshes, *Nature*, 403, 292-295, 10.1038/35002043, 2000.
- 515 Rhew, R. C., Aydin, M., and Saltzman, E. S.: Measuring terrestrial fluxes of methyl chloride and  
516 methyl bromide using a stable isotope tracer technique, *Geophys. Res. Lett.*, 30, 5, 2003.
- 517 Saito, T., and Yokouchi, Y.: Stable carbon isotope ratio of methyl chloride emitted from glasshouse-  
518 grown tropical plants and its implication for the global methyl chloride budget, *Geophys. Res. Lett.*,  
519 35, 2008.



- 520 Saueressig, G., Crowley, J. N., Bergamaschi, P., Brühl, C., Brenninkmeijer, C. A. M., and Fischer, H.:  
521 Carbon 13 and D kinetic isotope effects in the reactions of CH<sub>4</sub> with O(1D) and OH: New laboratory  
522 measurements and their implications for the isotopic composition of stratospheric methane, *Journal of*  
523 *Geophysical Research: Atmospheres*, 106, 23127-23138, 10.1029/2000JD000120, 2001.
- 524 Schafer, H., Miller, L. G., Oremland, R. S., and Murrell, J. C.: Bacterial cycling of methyl halides, in:  
525 *Advances in Applied Microbiology*, *Advances in Applied Microbiology*, 307-346, 2007.
- 526 Sellevåg, S. R., Nyman, G., and Nielsen, C. J.: Study of the Carbon-13 and Deuterium Kinetic Isotope  
527 Effects in the Cl and OH Reactions of CH<sub>4</sub> and CH<sub>3</sub>Cl, *The Journal of Physical Chemistry A*, 110,  
528 141-152, 10.1021/jp0549778, 2006.
- 529 Spence, J. W., Hanst, P. L., and Gay, B. W.: Atmospheric Oxidation of Methyl Chloride Methylene  
530 Chloride, and Chloroform, *Journal of the Air Pollution Control Association*, 26, 994-996,  
531 10.1080/00022470.1976.10470354, 1976.
- 532 Thompson, A. E., Anderson, R. S., Rudolph, J., and Huang, L.: Stable carbon isotope signatures of  
533 background tropospheric chloromethane and CFC113, *Biogeochemistry*, 60, 191-211, 2002.
- 534 Umezawa, T., Baker, A. K., Brenninkmeijer, C. A. M., Zahn, A., Oram, D. E., and van Velthoven, P.  
535 F. J.: Methyl chloride as a tracer of tropical tropospheric air in the lowermost stratosphere inferred  
536 from IAGOS-CARIBIC passenger aircraft measurements, *Journal of Geophysical Research:*  
537 *Atmospheres*, 120, 12,313-312,326, 10.1002/2015JD023729, 2015.
- 538 Urey, H. C.: Oxygen Isotopes in Nature and in the Laboratory, *Science*, 108, 489-496,  
539 10.1126/science.108.2810.489, 1948.
- 540 Vannelli, T., Messmer, M., Studer, A., Vuilleumier, S., and Leisinger, T.: A corrinoid-dependent  
541 catabolic pathway for growth of a *Methylobacterium* strain with chloromethane, *Proceedings of the*  
542 *National Academy of Sciences*, 96, 4615-4620, 10.1073/pnas.96.8.4615, 1999.
- 543 Westaway, K. C.: in: *Isotopes in organic chemistry, vol. 8: Secondary and solvent isotope effects*,  
544 edited by: Buncl, E., and Lee, C. C., Elsevier, Amsterdam, Oxford, New York, Tokyo, 275-392,  
545 1987.
- 546 Williams, J., Wang, N.-Y., Cicerone, R. J., Yagi, K., Kurihara, M., and Terada, F.: Atmospheric  
547 methyl halides and dimethyl sulfide from cattle, *Glob. Biogeochem. Cycle*, 13, 485-491,  
548 10.1029/1998GB900010, 1999.
- 549 Wittmer, J., Bleicher, S., and Zetzsch, C.: Iron(III)-induced activation of chloride and bromide from  
550 modeled salt pans, *The journal of physical chemistry. A*, 119, 4373-4385, 10.1021/jp508006s, 2015.
- 551 WMO: *Scientific Assessment of Ozone Depletion: 2010*, Global Ozone Research and Monitoring  
552 Project-Report No. 52, 516 pp., Geneva, Switzerland, 2011.
- 553 Xiao, Y., Tanaka, N., and Lasaga, A.: An evaluation of hydrogen kinetic isotope effect in the reaction  
554 of CH<sub>4</sub> with OH free radical (abstract). In: *Eos Trans. AGU*, 74, Spring Meet. Suppl., 71., 1993.
- 555 Yokouchi, Y., Ikeda, M., Inuzuka, Y., and Yukawa, T.: Strong emission of methyl chloride from  
556 tropical plants, *Nature*, 416, 163-165, 2002.
- 557 Yokouchi, Y., Saito, T., Ishigaki, C., and Aramoto, M.: Identification of methyl chloride-emitting  
558 plants and atmospheric measurements on a subtropical island, *Chemosphere*, 69, 549-553, 2007.  
559
- 560
- 561



562 Table 1: Reported hydrogen isotope enrichment constants for the reaction of CH<sub>3</sub>Cl with OH  
 563 radicals and with Cl atoms and the reaction of CH<sub>4</sub> with OH radicals.

Reaction	$\epsilon / \text{mUr}$	Method and remarks	Reference
CH <sub>3</sub> Cl + OH	-242	mean experimental: 3.5 m <sup>3</sup> smog-chamber at 293 ± 1 K; IRMS	Exp. 1 & 2, this study
CH <sub>3</sub> Cl + OH	-410 ± 50	experimental: smog-chamber, long-path FTIR spectroscopy relative to CH <sub>3</sub> Cl at 298 ± 2 K	Sellavåg et al. 2006
CH <sub>3</sub> Cl + OH	-330 to -430	theoretical calculations	Sellavåg et al. 2006
CH <sub>3</sub> Cl + Cl	-280 ± 11	experimental: 3.5 m <sup>3</sup> smog-chamber at 293 ± 1 K; IRMS	Exp. 3, this study
CH <sub>3</sub> Cl + Cl	-420 ± 40	experimental: smog-chamber, long-path FTIR spectroscopy relative to CH <sub>3</sub> Cl at 298 ± 2 K	Sellavåg et al. 2006
CH <sub>3</sub> Cl + Cl	-540 to -590	theoretical calculations	Sellavåg et al. 2006
CH <sub>4</sub> + OH	-205 ± 6	experimental: 3.5 m <sup>3</sup> smog-chamber at 293 ± 1 K; IRMS	Exp. 4, this study
CH <sub>4</sub> + OH	-227 ± 11	experimental: at 296 K, IRMS and tunable diode laser absorption spectroscopy	Saueressig et al. 2001
CH <sub>4</sub> + OH	-231 ± 45	experimental: at 277 K	Gierczak et al., 1997
CH <sub>4</sub> + OH	-251 ± 10	ab initio at 298 K	Xiao et al., 1993
CH <sub>4</sub> + OH	-145 ± 30	experimental: at 298 K	DeMore et al., 1993
CH <sub>4</sub> + OH	-294 ± 18	experimental: smog-chamber, long-path FTIR spectroscopy relative to CH <sub>3</sub> Cl at 298 ± 2 K	Sellavåg et al. 2006
CH <sub>4</sub> + OH	-60 to -270	theoretical at 298 K	Sellavåg et al. 2006



**Table 2.** Known sources of tropospheric CH<sub>3</sub>Cl and corresponding δ<sup>2</sup>H values.

Sources	Source (best estimate) <sup>a</sup> (Gg yr <sup>-1</sup> )	Source (full range) <sup>a</sup> (Gg yr <sup>-1</sup> )	Mean δ <sup>2</sup> H value mUr vs VSMOV	Uncertainty δ <sup>2</sup> H value ± mUr
Open field biomass burning	355	142 to 569	-236 <sup>b</sup>	44
Biomass burning indoor	113	56 to 169	-236 <sup>b</sup>	44
Tropical and subtropical plants	2040	1430 to 2650	-202 <sup>c</sup>	10
Fungi	145	128 to 162	?	
Salt marshes	85	1.1 to 170	?	
Coal combustion	162	29 to 295	?	
Industrial chemical production <sup>d</sup>	363	278 to 448	-130 <sup>e</sup>	20
Oceans	700	510 to 910	?	
Others <sup>f</sup>	-58	27 to 86	?	
<b>Total sources</b>	<b>3658 (4021)</b>	<b>2601 to 5459</b>		

<sup>a</sup> Values for source (best estimate) and source (full range) were taken from Carpenter and Reimann (2014), except for emissions associated with chemical production by the industry which are from Li et al. (2016). Value shown for total sources in brackets includes chemical production by the industry.

<sup>b</sup> Greule et al. (2012); please note that all values provided for CH<sub>3</sub>Cl released from dried plants at elevated temperatures have been corrected by -23 mUr due to recalibration of the reference gas.

<sup>c</sup> Jaeger et al. (2018b)

<sup>d</sup> Li et al. (2016)

<sup>e</sup> taken from Greule et al. (2012), Nadalig et al. (2013) and Jaeger et al. (2018a & 2018b); please note that values provided by Greule et al. (2012) and Nadalig et al. (2013) for CH<sub>3</sub>Cl from sources of the chemical industry have been corrected by -23 mUr due to recalibration of the reference gas

<sup>f</sup> including mangroves, wetlands, rice paddies and shrublands

? denotes that no value has been provided



**Table 3.** Known sinks of tropospheric CH<sub>3</sub>Cl and the mean isotope enrichment constant  $\epsilon$  reported for each.

Sinks	Sink (best estimate) <sup>a</sup> (Gg yr <sup>-1</sup> )	Sink (full range) <sup>a</sup> (Gg yr <sup>-1</sup> )	Isotope enrichment constant $\epsilon$ / mUr	Uncertainty $\epsilon$ $\pm$ mUr
Reaction with OH in troposphere	2832	2470 to 3420	-242 <sup>b</sup> -410 <sup>c</sup>	7 <sup>b</sup> 50 <sup>c</sup>
Loss to stratosphere	146	?	0 <sup>c</sup>	?
Reaction with Cl in marine boundary layer	370 <sup>d</sup>	180 to 550 <sup>d</sup>	-280 <sup>b</sup> -420 <sup>c</sup>	11 <sup>b</sup> 40 <sup>c</sup>
Microbial degradation in soil	1058	664 to 1482	-50 <sup>e</sup>	13 <sup>e</sup>
Loss in ocean	370	296 to 445	0 <sup>f</sup>	10 <sup>f</sup>
Microbial degradation in plants <sup>g</sup>	?	?	-8 <sup>g</sup>	19 <sup>g</sup>
Total sinks	4406 (4776)			

<sup>a</sup> Values for sink strength (best estimate and full range) were taken from Carpenter and Reimann (2014), except for the value of the reaction with Cl-radicals in marine boundary layer and for total sinks shown in brackets which includes the potential sink strength by Cl-radicals in marine boundary layer (Montzka and Fraser, 2003).

<sup>b</sup> this study, mean value of two experiments

<sup>c</sup> Sellevåg et al. (2006)

<sup>d</sup> Thompson et al. (2002) and discussion in this manuscript

<sup>e</sup> Jaeger et al. (2018a)

<sup>f</sup> Nadalig et al. (2014)

<sup>g</sup> Jaeger et al. (2018b)

? denotes that no value has been provided